Available online at www.sciencedirect.com
ScienceDirect
Clinical Biomechanics 23 (2008) 870–880
CLINICAL BIOMECHANICS
www.elsevier.com/locate/clinbiomech

Neuromuscular neutral zones response to static lumbar flexion: Muscular stability compensator

Jimmy Youssef [a,b], Bradley Davidson [a], Bing He Zhou [a], Yun Lu [a], Vikas Patel [a], Moshe Solomonow [a,b,*]

[a] *Musculoskeletal Disorders Research Lab, Bioengineering Division, Department of Orthopaedic Surgery, Health Sciences Center, University of Colorado, Denver, CO 80045, USA*
[b] *Department of Electrical Engineering, University of Colorado, Denver, CO 80045, USA*

Received 28 November 2007; accepted 26 March 2008

Abstract

Background. The impact of six sequential static loading and rest of the lumbar spine on the changes in the neuromuscular neutral zones and thereby on spine stability was assessed.

Methods. Six 10 min sessions of static load of a moderate level each spaced by 10 min rest were applied to the *in vivo* feline model. Test cycles of 0.25 Hz and at the same moderate peak load were applied before and every hour after the static loading sequence up to 7 h. Load, displacement and electromyographic activity of the lumbar multifidi muscles were recorded throughout.

Findings. Displacement and tension neuromuscular neutral zones were defined as the displacement or tension, in the increase and decrease phases of each cycle, when the electromyogram initiated and ceased activity, respectively. Displacement neuromuscular neutral zones demonstrated significant ($P < 0.001$) increase immediately post-static loading, followed by an exponential decrease to pre-loading baseline by the 7th hour. Tension neuromuscular neutral zones, however, demonstrated significant ($P < 0.001$) increase in the 2 h immediately after the static loading and a significant decrease ($P < 0.001$) thereafter. Peak electromyogram decreased in the first 3 h post-loading, but significantly ($P < 0.001$) increased thereafter to the 7th hour.

Interpretation. It was concluded that the first 2–3 h post-static loading finds the spine with significant laxity in the viscoelastic tissues concurrently with deficient muscular activation and therefore exposed to the risk of instability. It is also evident that a neural control compensation mechanism exists where it enhances the activation of the musculature to earlier and at higher activation magnitude, 2–3 h post-loading, increasing lumbar stability while the viscoelastic tissues are still lax.

Keywords: Spine; Lumbar; Stability; EMG; Muscle

1. Introduction

Spinal stability is a multifactoral problem, the extent of which is slowly emerging (Adams, 2007; Reeves et al., 2007). Panjabi (1992, 1996) hypothesized that a key structural component in spinal stability is that of neutral zones (NZ). By definition, a small perturbation of the vertebrae relative to adjacent vertebrae meets very little resistance from the various viscoelastic tissues (ligaments, discs, facet capsules, etc.) and in that region of displacement, the spine is considered structurally stable. Displacements beyond that region – the neutral zone – meet a fast increase in resistance as the spine becomes unstable and in need of support from the viscoelastic tissues.

Recently, the structural stability defined by the neutral zones was linked with contribution of the motor control system. In this approach, the neuromuscular neutral zone (NNZ) was defined as the amount of displacement or tension applied to the lumbar spine before reflexively triggered muscle activity increases the stiffness of the inter-vertebral

* Corresponding author. Address: Musculoskeletal Disorders Research Laboratory, Health Sciences Center, University of Colorado, Denver, 12800 E. 19th Avenue, Mail Stop 8343, P.O. Box 6511, Aurora, CO 80045, USA.
E-mail address: moshe.solomonow@uchsc.edu (M. Solomonow).

0268-0033/$ - see front matter © 2008 Elsevier Ltd. All rights reserved.
doi:10.1016/j.clinbiomech.2008.03.069

joints to maintain stability (Eversull et al., 2001; Solomonow et al., 2001). To date, it has been shown that NNZ magnitude is dependent on the rate of displacement or tension loading; smaller NNZs and an increase in peak electromyogram (EMG) amplitude of the multifidus muscle were observed at higher loading rates during spinal loading that approximated a flexion–extension movement. Furthermore, the NNZ during flexion was demonstrated to be smaller than the NNZ during the return extension.

Several epidemiological studies have shown static loading of the spine to be a risk factor for developing low back disorders (Hoogendoorn et al., 2000; Marras, 2000; Punnett et al., 1991). Recent experimental investigations have offered biomechanical and neurophysiologic validation in the feline model (Courville et al., 2005; LaBry et al., 2004; Sbriccoli et al., 2004a,b, 2007), and humans (Dickey et al., 2003; Granata et al., 1999, 2005; Krajcarski & Wells, 2006; Li et al., 2007; Little and Khalsa, 2005; Olson et al., 2004, 2006, in press; Shin and Mirka, 2007; Solomonow et al., 2003a). The emerging experimental data have demonstrated that creep develops in the lumbar viscoelastic tissues during prolonged static flexion (Adams et al., 1987; Hedman and Fernie, 1995; Keller et al., 1988; McGill and Brown, 1992; Solomonow et al., 1999; Twomey and Taylor, 1982) and that it is associated with observed spasms in the multifidus, decreased reflexive muscular activity during work and two stages of hyperexcitability during the hours after loading. Development of acute inflammation and a neuromuscular disorder have been observed for periods of high static loads, insufficient rest between work sessions, large number of repetitions, and long work duration (Courville et al., 2005; LaBry et al., 2004, Sbriccoli et al., 2007; Solomonow et al., 2003b). Such pronounced changes in the biomechanical and motor control properties of the lumbar spine may also have significant implications on the NNZ after a period of static loading.

Therefore, the purpose of this study was to investigate potential changes in the NNZ after prolonged static lumbar loading. We hypothesized that displacement and tension NNZs would increase following a session that included periods of static lumbar loading separated by equal periods of rest, and that several hours of rest would be necessary for the NNZs to return to baseline (pre-static loading levels). We also hypothesized that changes would occur in the EMG amplitude following static loading and during several hours of following rest. The results of this investigation may provide important new insight into the changes in the stability of the lumbar spine after static work, injury potential and possible prevention, and baseline data for designing safe work scheduling.

2. Methods

2.1. Preparation

Eight adult cats (weight: 3.34 ± 0.51 kg) were used in this study. The cats were anesthetized with 60 mg/kg chloralose, according to a protocol approved by the Institutional Animal Care and Use Committee. The skin overlying the lumbar spine was incised to expose the dorso-lumbar fascia, and an S-shaped stainless steel hook made of 1.5-mm-diameter rod was inserted around the supraspinous ligament between L_4 and L_5. The preparation was then positioned in a rigid stainless steel frame and fixed for subsequent EMG electrode insertion. The lumbar spine was isolated by means of two external fixators applied to the L_1 and L_7 posterior processes, respectively. The external fixation was intended to isolate the elicited flexion to the lumbar spine and prevent interaction with the thoracic, sacral, and pelvic structures.

2.2. Instrumentation

Three pairs of fine stainless steel wire EMG electrodes (interelectrode distance: 3–4 mm) were inserted in the right $L_{3–4}$, $L_{4–5}$, and $L_{5–6}$ multifidus muscles 6–8 mm lateral to the posterior spinal processes. A ground electrode was inserted into the gluteus muscle. Each electrode pair constituted the input to a differential EMG amplifier with a 110-dB common mode rejection ratio, a gain of up to 200,000, and a band-pass filter in the range of 6–500 Hz. The EMG was sampled at 1000 Hz before storage on a computer and continuously monitored on an oscilloscope. The S-shaped stainless steel hook inserted around the $L_{4–5}$ supraspinous ligament was connected to the crosshead of the Bionix 858 Material Testing System (MTS, Minneapolis, MN, USA). The load was applied through the MTS actuator with a computer-controlled loading system. Vertical displacement and tension applied to the hook around the supraspinous ligament were continuously monitored, and sampled at 1000 Hz before storage on a computer.

2.3. Protocol

Just prior to each test cycle or static load, a pretension of 1 N was applied to standardize the baseline tension across all preparations. First, the baseline NNZs were established using three pre-static loading test cycles of 40 N peak load at 0.25 Hz. The test cycles were applied with a 10 min rest (no load) between each. A peak load of 40 N was selected, as it represents a moderate load in the physiological range as was determined in previous research (Sbriccoli et al., 2004a). Next, a static loading period was applied that consisted of six 10 min static loads at 40 N, each separated by 10 min periods of rest, resulting in a cumulative static loading period of 60 min. A recovery period after static loading followed and consisted of 7 h rest (no load). Single test cycles identical to those before the static loading session were applied at 10 min, 30 min, and 60 min, and then once every hour during the recovery period. Overall, nine test cycles were applied during the 7-h recovery as shown graphically in the bottom panel of Fig. 1.

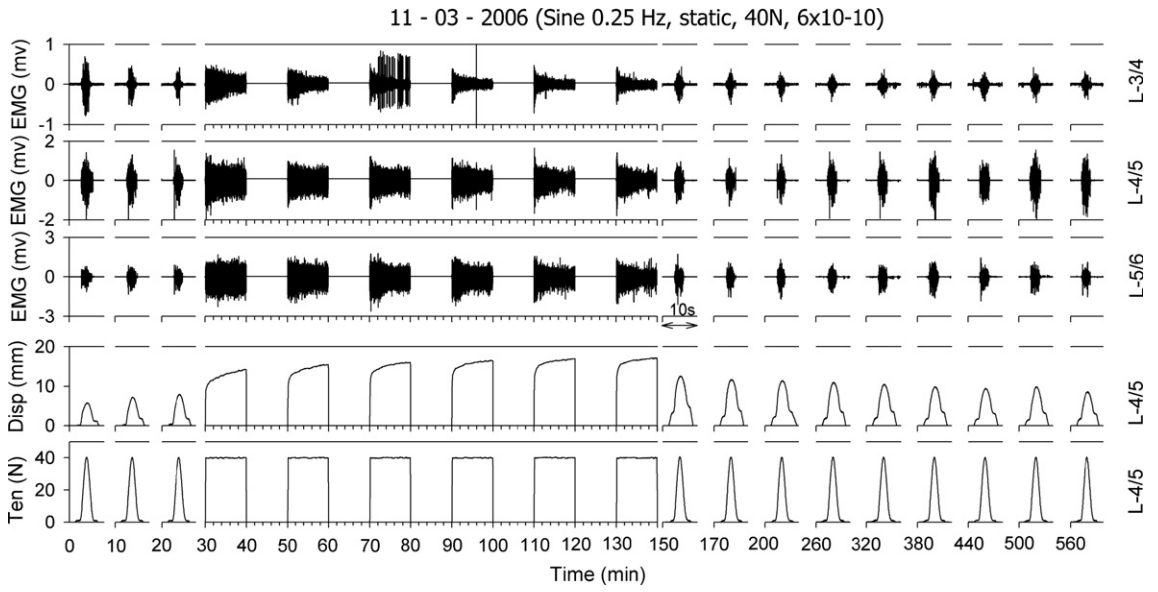

Fig. 1. A typical recording of the EMG from L_{3-4}, L_{4-5}, and L_{5-6} vertebral levels along with the displacement and tension. Three test cycles were applied before the static loading period (consisting of six static loads with rest periods between) and nine test cycles were applied during the 7 h recovery period. Note: The creep developing and accumulating during the static loading phases and the spontaneous large amplitude EMG spasms such as in the L_{3-4} level.

2.4. Data processing

The NNZ analysis considered the recorded EMG, displacement, and tension applied to the supraspinous ligament during the three test cycles prior to the static loading session and the nine test cycles during the 7 h recovery period. Each test cycle was analyzed in a 5 s window that consisted of 0.5 s before and 0.5 s after the 4 s cycle (0.25 Hz). The EMG signal was conditioned in the following manner: EMG recorded from each lumbar level were full-wave-rectified, and a moving window of 200 ms was smoothed with a 200 ms low-pass filter, followed by similar smoothing of the next 200 ms window moved up 10 sampling points along the time axis, thereby, obtaining the Mean Absolute Value (MAV) of each EMG channel without creating a time delay. The mean MAV of the first 500 ms of each 5 s window, which occurred before the loading was initiated, was used as the baseline MAV. After the tension was applied, muscle activation onset was considered to be when the MAV exceeded three times the baseline value. Three times baseline value was chosen in order to avoid false identification of NNZ due to spontaneous action potentials which are common in resting EMG. The corresponding displacement and tension values during the stretch phase (increasing tension) of the cycle were recorded as the onset displacement neuromuscular neutral zone (DNNZ) and the onset tension neuromuscular neutral zone (TNNZ), respectively. When the EMG signal dropped below three times the baseline MAV during the relaxation (decreasing tension) phase of the cycle, the corresponding displacement and tension were recorded as the offset DNNZ and TNNZ, respectively. This procedure was visually supervised to ensure that signal artifacts were not detected as thresholds.

The maximum MAV value from each loading cycle was denoted as the peak MAV. The peak MAV from the three pre-static loading cycles were averaged together and used to normalize the peak MAV values in the cycles of the same preparation during the 7 h recovery period.

2.5. Statistics

The DNNZ and TNNZ from the three pre-static loading cycles were averaged together to give a baseline value for each dependent variable. A three-way repeated measures ANOVA was used to test for differences in the stretch and relaxation phases of the DNNZ and TNNZ. The independent variables included time (pre-static loading, recovery times), lumbar level of the multifidus (L_{3-4}, L_{4-5}, L_{5-6}), and loading phase (stretch, relaxation). All the dependent variables were tested for changes in time and lumbar level with a two-way repeated measures ANOVA. The independent variables were time (pre-static loading, recovery times) and lumbar level of the multifidus (L_{3-4}, L_{4-5}, L_{5-6}), and the dependent variables included both stretch phase and relaxation phase thresholds for the DNNZ and TNNZ and peak MAV. All higher order factorial terms were included in the statistical models to test for interaction of the independent variables. Upon determining a significant interaction or main effect, pair-wise comparisons were performed using a Student *t*-test. Level of significance was set as $P = 0.05$.

2.6. Modeling

The mean ± SD values of the DNNZ, TNNZ, and peak MAV during recovery for each lumbar level were fit with

exponential-based models, as they represent the classical response of viscoelastic tissues (Solomonow et al., 2000).

The time-course of the DNNZ thresholds during the stretch phase and relaxation phase of the test cycles during the recovery period were described by

$$\mathrm{DISP}(t) = D_0 + D_R + (D_L - D_R)(e^{-\frac{t-\tau_r}{\tau_1}}) \quad \{t|150 \leqslant t \leqslant 560\}, \tag{1}$$

where

- D_0 is the steady-state displacement (mm);
- D_L is the amplitude of the exponential decay (mm);
- D_R is the residual creep after recovery (mm);
- t is time measured since the beginning of the experiment (min);
- τ_1 is the exponential time constant (min);
- τ_r is the time of the first recovery measurement (150 min).

As noted above, the model was evaluated from the time point of 150 min to 560 min, which constitute the 7 h of recovery post-static loading.

The time-course of the TNNZ thresholds during the stretch phase and relaxation phase of the test cycles during the recovery period were described by

$$\mathrm{TEN}(t) = T_0 + (t-\tau_r)T_L\left(e^{-\frac{t-\tau_r}{\tau_2}}\right) + T_M\left(e^{-\frac{t-\tau_r}{\tau_3}}\right) \quad \{t|150 \leqslant t \leqslant 560\}, \tag{2}$$

where

- T_0 is the intercept of the tension (N);
- T_L affects the rise amplitude (N/s);
- T_M is the amplitude of the decay dominating the end of the recovery period (N);
- $(t-\tau_r)T_L e^{-(t-150)/\tau_2}$ allows for a transient rise at the beginning of the recovery period;
- τ_2 affects the rates of rise and fall (s);
- τ_3 is the exponential time constant of the decay that dominates the end of the recovery period (min).

The time-course of the peak MAV during the recovery period were described by

$$\text{peak MAV}(t) = P_0 + P_L(e^{-\frac{t-\tau_r}{\tau_4}}) + P_M(1 - e^{-\frac{t-\tau_r}{\tau_5}}) + (t-\tau_d)P_H(e^{-\frac{t-\tau_d}{\tau_6}}) \quad \{t|150 \leqslant t \leqslant 560\}, \tag{3}$$

where

- P_0 is the intercept of the peak MAV (mm);
- P_L is the amplitude of the exponential decay (mm);
- P_M is the amplitude of the exponential increase (mm);
- t is time measured since the beginning of the experiment (min);
- τ_4, τ_5 are exponential time constants (min);
- τ_r is the time of the first recovery measurement (150 min);
- $(t-\tau_d)P_H e^{-\frac{t-\tau_d}{\tau_6}}$ is the hyperexcitability term. This term has a delayed onset during the recovery period and is equal to zero when $t < \tau_d$.

Levenberg–Marquardt nonlinear regression algorithms were used to generate the best fit models, optimizing for regression coefficient.

3. Results

A typical recording of the raw EMG taken from L_{3-4}, L_{4-5} and L_{5-6}, along with the measured displacement and tension from the three pre-static loading test cycles, static loading period, and nine test cycles during the recovery period is shown in Fig. 1. EMG, MAV, tension and displacement recorded during a typical test cycle are shown in Fig. 2 as well as the arrows denoting the initiation and cessation of EMG.

3.1. Displacement neuromuscular neutral zone (DNNZ)

Fig. 3 shows the mean (SD) of the DNNZ for the first three cycles and the nine test cycles during recovery. The

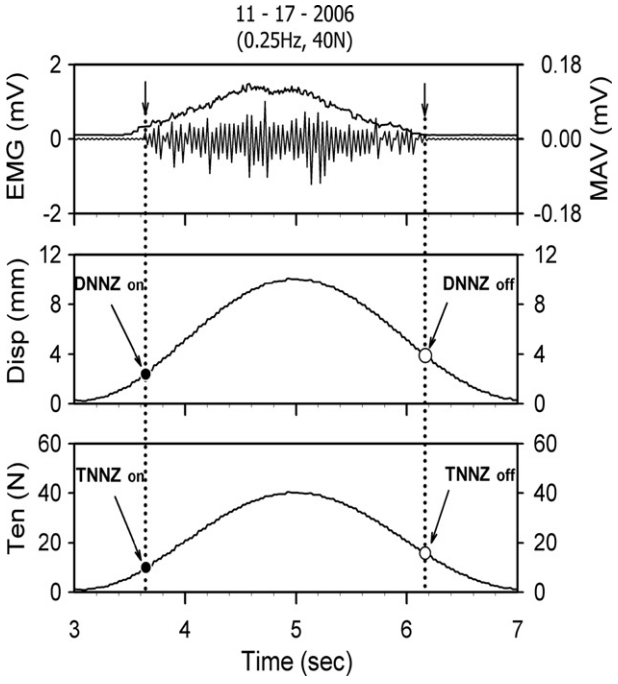

Fig. 2. Typical response to a single cycle of load from one preparation. The top trace show the raw EMG from the three lumbar levels with the associated mean absolute value (MAV) superimposed. The second trace from the top shows the displacement and the bottom trace shows the tension. The arrows shown on the EMG traces denote the onset and offset of the EMG. The vertical projections of the arrows into the displacement and load traces determine the corresponding displacement and tension neuromuscular neutral zones. The solid circles denote in NNZ during flexion and the hollow circles show the NNZ during extension.

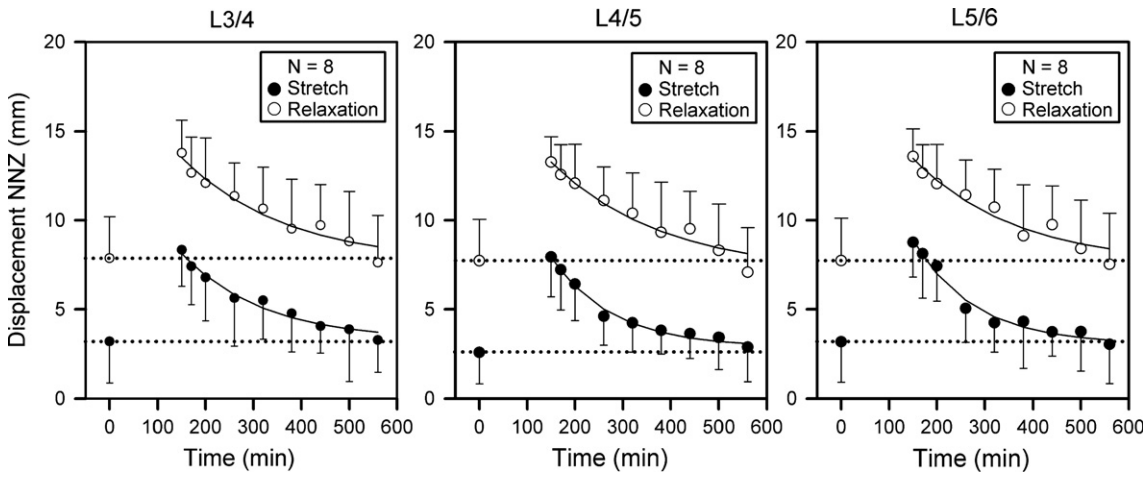

Fig. 3. The mean (SD) displacement neuromuscular neutral zones (DNNZs) during the stretch and relaxation phases of the cycle, before the static loading period and during the 7 h recovery period. The resulting exponential-based model is superimposed on the plot.

mean(SD) of the baseline DNNZ during the stretch phase of the test cycle were 3.18(SD 2.3) mm, 2.57(SD 1.75) mm, and 3.16(SD 2.25) mm for the L_{3-4}, L_{4-5}, and L_{5-6} levels, respectively. The DNNZ during stretch of the three lumbar levels demonstrated significant differences with time ($P < 0.001$) in that they increased nearly three fold following the static loading period to 8.33(SD 2) mm, 7.94(SD 2.24) mm, and 8.76(SD 1.95) mm, and remained significantly elevated to the sixth hour into the recovery period. The final DNNZ during stretch were 3.26(SD 1.8) mm, 2.87(SD 1.9) mm and 3.03(SD 2.18) mm for the L_{3-4}, L_{4-5}, and L_{5-6}, respectively. DNNZ during stretch for L_{4-5} was significantly lower ($P = 0.009$) than those in L_{3-4} and L_{5-6}. A time and vertebral level interaction was not present ($P = 0.989$).

The baseline DNNZ during the relaxation phase of the test cycle were 7.87(SD 2.3) mm, 7.72(SD 2.3) mm and 7.73(SD 2.38) mm for the L_{3-4}, L_{4-5}, and L_{5-6} levels, respectively. The DNNZ of the three lumbar levels during relaxation demonstrated significant differences with time ($P < 0.001$) in that they nearly doubled following the static loading period to 13.8(SD 1.8), 13.2(SD 1.4), and 13.58(SD 1.6), and remained significantly elevated to the fifth hour into the recovery period. The final DNNZ during relaxation were 7.62(SD 2.6), 7.07(SD 2.5) and 7.52(SD 2.8) for the L_{3-4}, L_{4-5} and L_{5-6} levels, respectively. Differences across vertebral level ($P = 0.363$) or time and vertebral level interaction ($P = 1.000$) were not present.

The DNNZ during relaxation were significantly higher ($P < 0.001$) than their corresponding DNNZ during stretch, before and after the static loading.

3.2. Tension neuromuscular neutral zone (TNNZ)

The mean ± SD of the TNNZ before and after the static loading are shown in Fig. 4. The baseline TNNZ thresholds during the stretch phase of the test cycle were 9.86(SD 5.7) N, 7.85(SD 4.8) N, and 9.18(SD 5.2) N for the L_{3-4}, L_{4-5}, and L_{5-6} levels, respectively. The TNNZ during stretch demonstrated a significant effect of time

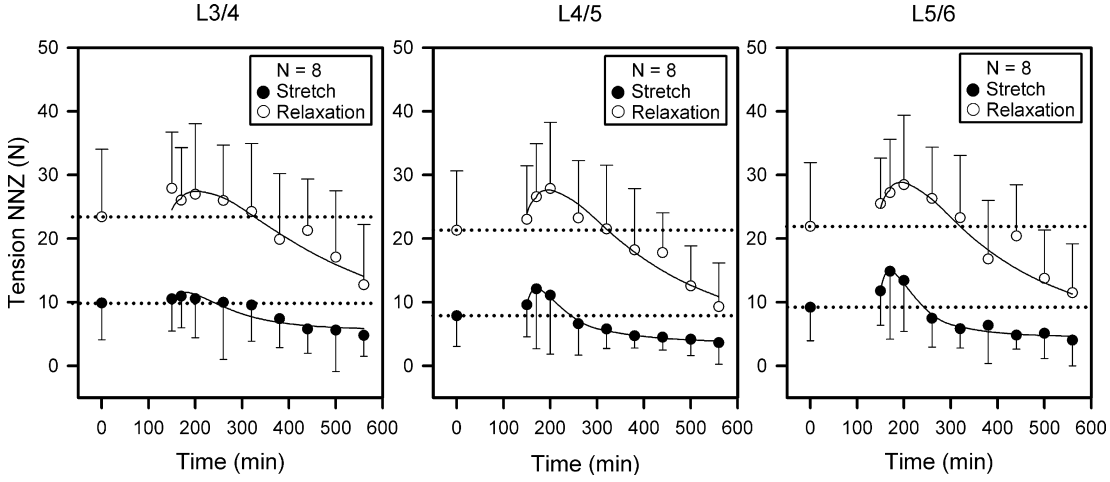

Fig. 4. The mean (SD) tension neuromuscular neutral zones (TNNZs) during the stretch and relaxation phases of the cycle, before the static loading period and during the 7 h recovery period. The resulting exponential-based model is superimposed on the plot.

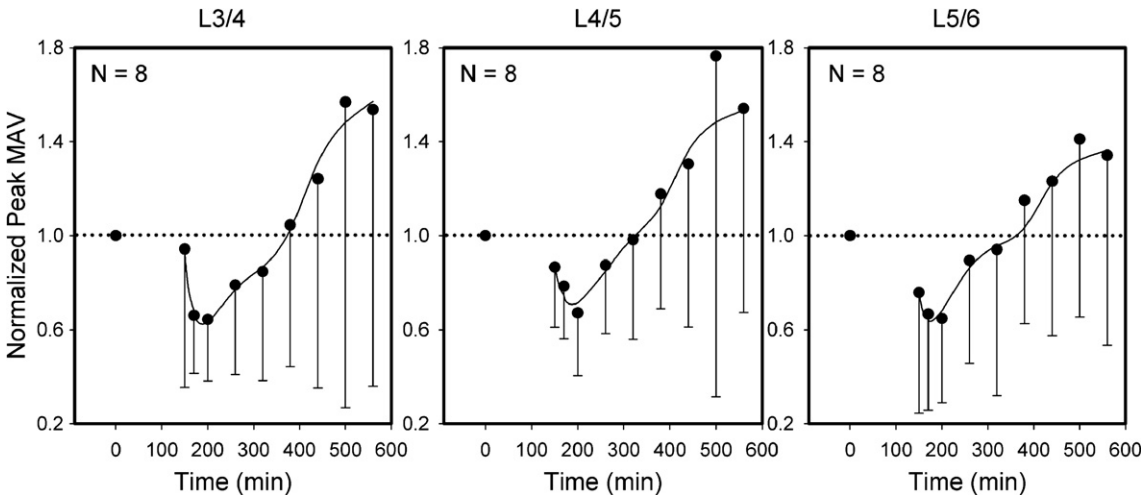

Fig. 5. The mean (SD) normalized peak mean absolute values (PMAVs) during the stretch and relaxation phases of the cycle, before the static loading period and during the 7 h recovery period. Note the region of significant increase beginning around minute 320. The resulting exponential-based model is superimposed on the plot.

($P < 0.001$), which included an increase that occurred at 30 min into the recovery period and a decrease below the baseline after 2 h into the recovery period. The final TNNZ during stretch were 7.62(SD 2.6) N, 7.07(SD 2.5) N and 7.52(SD 2.8) N for the L_{3-4}, L_{4-5} and L_{5-6} levels, respectively. When pooled across vertebral level, the final TNNZ was 48.6(SD 29.9)% lower than baseline. The TNNZ for L_{4-5} was significantly lower ($P = 0.010$) than those in L_{3-4} and L_{5-6}. A time and vertebral level interaction was not present ($P = 0.971$).

The baseline TNNZ during the relaxation phase of the test cycle were 23.4(SD 10.6) N, 21.3(SD 9.3) N, and 21.9(SD 10) N for the L_{3-4}, L_{4-5}, and L_{5-6} levels, respectively. The TNNZ during relaxation of the three lumbar levels demonstrated significant differences with time ($P < 0.001$) in that they increased during the first hour into the recovery period. Measurements at 2 h and 3 h into the recovery period demonstrated no significant difference from baseline. After the third hour into the recovery period, the TNNZ threshold significantly decreased below the baseline throughout the remainder of the recovery period. The final TNNZ during relaxation were 12.7(SD 9.5) N, 9.27(SD 6.8) N and 11.5(SD 7.7) N for the L_{3-4}, L_{4-5} and L_{5-6} lumbar levels, respectively. When pooled across vertebral level, the final value was 51.6(SD 25)% lower than the baseline thresholds. TNNZ relaxation threshold for L_{4-5} was lower ($P = 0.020$) than the threshold in L_{3-4}. A time with vertebral level interaction was not present ($P = 0.998$).

The TNNZ during relaxation were significantly higher ($P < 0.001$) than their corresponding TNNZ during stretch, before and after static loading.

3.3. EMG peak mean absolute value

(Fig. 5) shows the peak mean absolute value of the EMG before and after the static loading. During the recovery period, the peak MAV demonstrated an initial decrease below the baseline values during the first hour and then gradually increased to levels exceeding the baseline after the third hour. The peak MAV demonstrated significant changes with time ($P < 0.001$) as seen in the 33.7(SD 28.4)% (average change in the three muscle sites) reduction below the baseline within 1 h after the static loading period ended, and then rising as high as 58.1(SD 116.1)% above baseline at 6 h into the recovery period. Differences across vertebral level ($P = 0.526$) or time with vertebral level interaction ($P = 1.000$) were not present.

3.4. Models

The exponential models derived for the DNNZ, TNNZ, and peak MAV are superimposed on the experimental data in Figs. 3–5, and the corresponding model parameters are given in Tables 1–3.

The time-course of the DNNZ during the recovery period was modeled with a single exponential decay at each vertebral level. Regression coefficient (r^2) for the models representing the DNNZ ranged from 0.95 to 0.99. The amplitudes of exponential decay, D_L, were similar across vertebral level and also between the stretch and relaxation

Table 1
Displacement NNZ model $DNNZ(t) = D_0 + D_R + (D_L - D_R)e^{-[(t-\tau_R)/\tau_1]}$

	Stretch			Relaxation		
	L3/L4	L4/L5	L5/L6	L3/L4	L4/L5	L5/L6
D_0	3.18	2.57	3.16	7.87	7.72	7.72
D_R	0.082	0.293	−0.141	−0.252	−0.648	−0.207
D_L	4.95	5.36	5.75	5.65	5.56	5.75
τ_1	170.5	127.6	126.9	217.0	231.6	213.6
r^2	0.9813	0.9876	0.9767	0.9709	0.9739	0.9524

Model parameters for displacement neuromuscular neutral zone thresholds during the recovery period. The stretch and relaxation phases of loading denotes the onset of and offset of the EMG signal, respectively.

Table 2
Tension NNZ model $TNNZ(t) = T_0 + (t - \tau_R)T_L e^{-[(t-\tau_R)/\tau_2]} + T_M e^{-[(t-\tau_R)/\tau_3]}$

	Stretch			Relaxation		
	L3/L4	L4/L5	L5/L6	L3/L4	L4/L5	L5/L6
T_0	5.58	3.52	4.49	0.00	0.00	0.00
T_L	0.123	0.358	0.480	0.156	0.225	0.253
τ_2	50.1	27.9	27.8	100.7	80.6	74.2
T_M	4.84	6.00	7.16	24.5	23.9	24.7
τ_3	140.0	144.9	106.4	643.9	485.7	498.2
r^2	0.8645	0.9927	0.9831	0.8775	0.9468	0.8974

Model parameters for tension neuromuscular neutral zone thresholds during the recovery period. The stretch and relaxation phases of loading denotes the onset of and offset of the EMG signal, respectively.

Table 3
Peak MAV model. Peak $MAV(t) = P_0 + P_L e^{-[(t-\tau_R)/\tau_4]} + P_M(1 - e^{-[(t-\tau_R)/\tau_5]}) + (t - \tau_d)P_H e^{-[(t-\tau_d)/\tau_6]}$

	L3/L4	L4/L5	L5/L6
P_0	−8.069	−7.64	−5.57
P_L	9.00	8.52	6.33
τ_4	40.0	58.7	37.7
P_M	8.99	8.81	6.57
τ_5	43.8	65.1	42.0
τ_d	330.3	339.4	308.5
P_H	0.006	0.004	0.004
τ_6	287.4	230.0	233.5
r^2	0.9835	0.9175	0.9848

Model parameters for the EMG peak mean absolute value during the recovery period.

phases (stretch: 4.95–5.75 mm, relaxation: 5.56–5.75 mm). The time constants, τ_1, were lower in the stretch phase (126.9–170.5 min) than the relaxation phase (213.6–231.6 min).

The time-course of the TNNZ during the recovery period was modeled with two exponential terms, one with a linear multiplier and exponential decay and the other with only exponential decay, at each vertebral level. Regression coefficient (r^2) for the models representing the TNNZ ranged from 0.86 to 0.99. The linear multipliers, T_L, were generally higher for the stretch phase (0.123–0.480 N/min) than the relaxation phase (0.156–0.253 N/min). Conversely, the time constants, τ_2, in the same term were lower in the stretch phase (27.8–50.1 min) than the relaxation phase (74.2–100.7 min). In the decaying term that dominated the later part of the recovery period, the amplitudes of exponential decay, T_M, were lower during the stretch phase (4.84–7.16 N) than the relaxation phase (23.9–24.7 N). Conversely, the time constants, τ_3, for the stretch phase were lower (106.4–144.9 min) than the relaxation phase (485.7–643.9 min).

The initial time-course of the peak MAV during the recovery period was modeled at each vertebral level with two exponential terms, one decaying and one rising. The rising peak MAV in the later portion of recovery was modeled by adding a term with a linear multiplier and exponential decay after time τ_d. Regression coefficient (r^2) for the models representing the TNNZ ranged from 0.92 to 0.98. The exponential amplitudes, P_L and P_M, and time constants, τ_4 and τ_5, were similar in decay and rise as well as across vertebral level (exponential amplitudes: 6.33–9.00, time constants: 37.7–65.1). Amplitudes and time constants of the delayed term were similar across vertebral level (amplitudes, Ph: 0.004–0.006, time constant, T6: 230.0–287.4). Onsets of the rising exponential, τ_d, varied from 308.5 to 339.4 min.

Fig. 6 provides a summary of the percent increases/decreases in the DNNZ, TNNZ and peak MAV and the associated statistical significance over the 7 h recovery period.

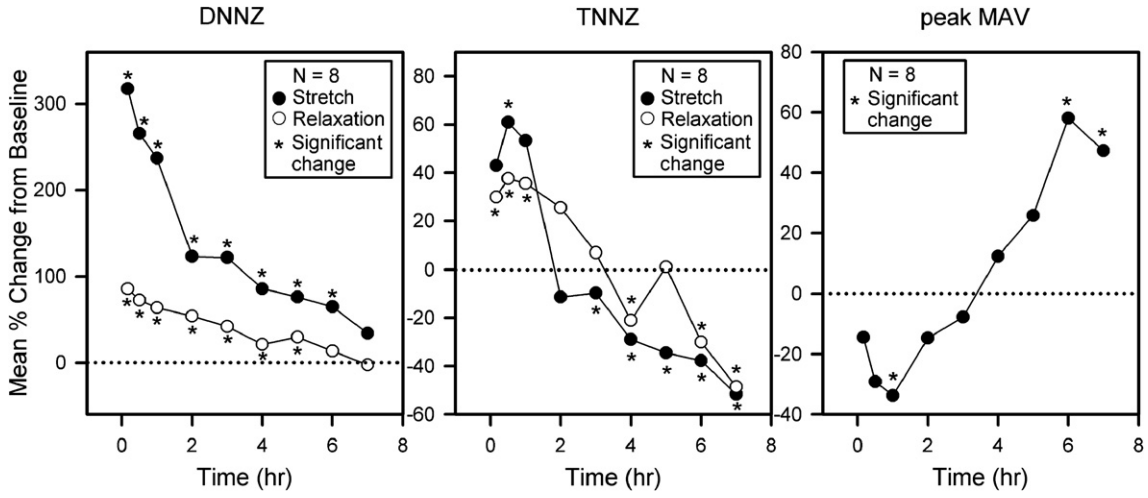

Fig. 6. Percent change compared to the baseline values for displacement neuromuscular neutral zone (DNNZ), tension neuromuscular neutral zone (TNNZ), and peak mean absolute value (MAV) of the EMG during the recovery period. Solid circles indicate EMG onset, and hollow circles indicate relaxation phase offset of EMG signal. Time zero indicates the end of the static loading period, and the asterisks denote a significant difference ($P < 0.05$) from baseline. Data is for the average (SD) across all three levels.

4. Discussion

The major findings of this investigation demonstrate that a period of static lumbar loading in flexion results in the development of laxity in the associated viscoelastic tissues, which in turn, elicit significant increases in the displacement and tension NNZ, compromising spinal stability in the post-loading period. Seven hours of rest, post-static loading, were required to restore the DNNZ to normal. Surprisingly, the TNNZ demonstrated a short increase for the first 2 h after loading, followed by a significant decrease thereafter. The peak MAV of the EMG from the multifidi also demonstrated a decrease in amplitude for the first 3 h post-loading, followed by a significant increase thereafter. Overall, while the viscoelastic tissues were lax after static loading and remained so for 7 h, a motor control mechanism compensated for the laxity by triggering the muscles earlier and with increased amplitude 2–3 h after the loading. A decreased lumbar stability consisting of laxity of the viscoelastic tissues concurrent with significantly delayed and decreased muscular activity were, nevertheless, noted in the first 2–3 h after the static loading. The 2–3 h post-static loading, therefore, presented a period of exposure to injury secondary to combined deficiency of viscoelastic tissues and the muscles to maintain inter-vertebral stability.

The large and significant post-loading increases in the DNNZs during the stretch (about 150%) and relaxation (86%) phases were relatively unsurprising. Static and cyclic loading have been repeatedly shown to induce creep in the passive viscoelastic tissues of the spine in normal humans (Dickey et al., 2003; Hedman and Fernie, 1995; McGill and Brown, 1992; Olson et al., 2004, 2006, in press), cadaveric specimens (Twomey & Taylor, 1982), and *in vivo* feline models (Courville et al., 2005; LaBry et al., 2004; Sbriccoli et al., 2004a,b; Solomonow et al., 1999). These results indicate that as laxity develops in the viscoelastic tissues, they must be stretched to longer lengths in order to excite the mechano-receptors and trigger the muscular reflexes (Stubbs et al., 1998). Therefore, neuromuscular activity after the static loading was not triggered until the displacements were much larger than before the static loading.

The increased laxity in the viscoelastic tissues persisted for several hours, as the DNNZ was not fully restored until the 7th hour of recovery. Over this time the lumbar spine did not benefit from the normal level of stiffness provided by these tissues, which potentially increased the risk of spinal instability with movement.

The gradual decreases in the DNNZs during the recovery period were fit well with models that included a single decaying exponential. This form represents the typical simplified creep recovery response of viscoelastic tissues such as ligaments and discs that contain viscous and elastic elements, (Solomonow et al., 2000) and has been used in previous investigations to model recovery of creep induced in the lumbar viscoelastic tissues (Courville et al., 2005; LaBry et al., 2004; Sbriccoli et al., 2004a,b; Solomonow et al., 1999). One key difference between the creep recovery and the DNNZ recovery is that the associated time constants are much larger for the recovery of the DNNZ for similar static loading magnitudes (DNNZ: 127–171 min (stretch), 214–232 min (relaxation); creep recovery: 35–45 min (LaBry et al., 2004; Sbriccoli et al., 2004b)). Although the DNNZ is certainly related to the viscoelastic creep in the supporting tissues, this drastic difference suggests that relying upon viscoelastic creep to approximate changes in the neutral zone may produce an artificially fast rate of recovery. The sharp increase in the muscular activity in the last 4 h of the recovery period tends to increase the stiffness of the lumbar spine and obscure the actual creep measurements.

Surprisingly, the TNNZs displayed a completely different behavior than the DNNZs. Following the static loading period, moderate increases in the TNNZs of 40% and 60% were observed within the first hour for the stretch and relaxation phases, respectively. The trend was reversed, and the TNNZs dropped below the baseline levels after the second hour of the recovery period and continue to decrease. This pattern is indicative of a temporarily increased risk of spinal instability, within the first 2 h following the static loading period, followed by a compensatory region where muscle activity was triggered at much lower tensions in the viscoelastic tissues. After the 3rd hour post-static loading, the tension at which the muscles triggered activity was 15% below baseline and up to 55% as additional time elapsed.

A visualization of the compensatory action of the TNNZ with respect to the DNNZ can be seen in Fig. 7. The left panel of Fig. 7 shows the baseline hysteresis collected from a test cycle before the static loading period and the hysteresis collected from a test cycle 1 h into the recovery period. Solid circles mark the NNZ during the stretch phase and the hollow circles mark the NNZ during the relaxation phase. The hysteresis recorded 1 h into the recovery period demonstrates a large increase in the DNNZs and TNNZs during the stretch and relaxation phases. In the middle panel, the baseline hysteresis is displayed on the same plot as the hysteresis recorded 2 h into the recovery period. It is clear that while the DNNZ during stretch phase remained elevated above the baseline DNNZ, the TNNZ during the stretch phase was nearly 50% smaller than the baseline TNNZ. In the right panel, the baseline hysteresis is displayed with the hysteresis recorded 6 h into the recovery period. This plot shows that the TNNZ during both the stretch and relaxation were well below the baseline TNNZ, even while the DNNZ had not fully recovered. Overall, these trends indicate that certain levels of independence from viscoelastic tissues laxity are exercised by the motor control system by reflexively activating the musculature at significantly lower tension thresholds, and providing stiffness that was absent in the lumbar spine due to increased intrinsic laxity.

The original ligamento-muscular reflex was shown to originate from mechano-receptors in the lumbar ligaments

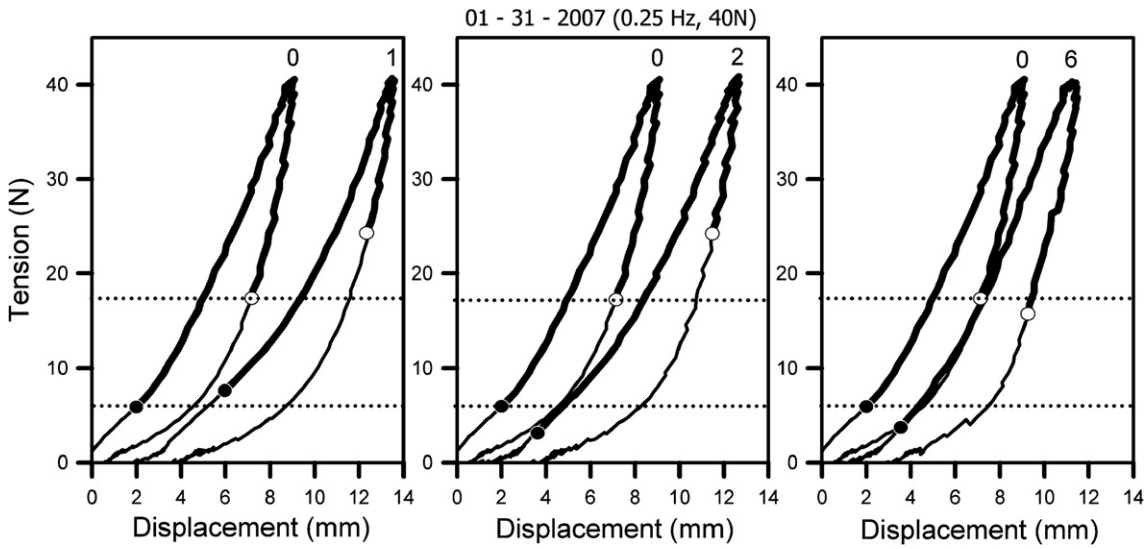

Fig. 7. Each panel shows a typical hysteresis recorded before the static loading period with a hysteresis collected during the recovery period. The curve labeled 0 – denotes the baseline test curve before the static loading, 1 – denotes the curve of the test cycle after 1 h of recovery post-loading, 2 – denotes the test cycle 2 h into the recovery, and 6 – denotes the test cycle 6 h into the 7 h recovery period. Solid circles mark the EMG onset during the stretch phase and the hollow circles mark the EMG offset during the relaxation phase. Note: The decrease of the TNNZ in the middle panel while the DNNZ was still substantially high and also in the right panel where the DNNZ is still not fully recovered.

to the multifidi muscles, with a decreasing EMG amplitude with the increased duration of flexion (Solomonow et al., 1999; Stubbs et al., 1998). The EMG was repeatedly observed to recover exponentially in parallel with the recovery of the creep (Courville et al., 2005; LaBry et al., 2004; Sbriccoli et al., 2004a,b, 2007). Since the TNNZ were triggered much earlier and out of synchronization with the DNNZ or creep, it is doubtful that the simple ligamento-muscular reflex was the source or the trigger. Most likely, a different compensatory motor control mechanism was the source of the early activation of the multifidi and the sharp decrease in the TNNZ.

Analysis of the peak MAV confirmed the compensatory effect due to the motor control component of spinal stabilization. Following the static loading period, the peak MAV decreased for the first hour and then increased throughout the remaining 6 h. After the third hour, the peak MAV exceeded the baseline values. Accounting for all of the variables in this investigation, we can conclude that in addition to the typical laxity that occurs after static loading, the motor control stabilizing mechanism is compromised as seen in the increased DNNZs and TNNZs as well as the decreased peak MAV. This period of compromised motor control, lasting from 2 to 3 h, likely exposes the spine to increased risk of destabilization and potential injury. Beyond this period, a neuromuscular compensatory mechanism is triggered. While the DNNZ is still significantly increased and deficient, the TNNZ significantly decreases up to 50% below the baseline values and triggers stabilizing muscle activity at nearly a 60% higher level than baseline values. This protective mechanism may be necessary to provide the needed stability while allowing creep recovery in the viscoelastic tissues. This compensatory motor control mechanism, therefore, consists of two components; activation of muscles at significantly lower tension in the viscoelastic tissues and at significantly higher activation magnitude.

The compensatory mechanism is consistent with both clinical and occupational findings. van Dieen et al. (2003) demonstrated that patients with compromised structural stability exhibit a high level of activation in the lumbar musculature and significant increase in stiffness. Likewise, it has been commonly observed that individuals sustain increased stiffness of the lumbar spine several hours after completing a period of work (Granata and Marras, 2000).

These findings raise several questions regarding this compensatory reaction: What is the neural monitoring mechanism that identifies periods of potential instability and elicits earlier muscular activity at a higher intensity? How long does the compensatory activity last? By what mechanism is the cessation of compensatory activity prompted?

Precise answers to such questions are presently unavailable; however, recent research with human subjects provides insight into the possible mechanism of the compensatory reaction. Olsen et al. (2004, in press) tested normal human subjects performing cyclic flexion–extension in passive and active conditions, as well as with various orientations with respect to the gravity vector. These tests indicated that reflexive muscular activity could be triggered or inhibited by the moment requirements on the spine. When the same flexion–extension motions were performed along with a different orientation with respect to gravity (and thereby its effect on the trunk mass), the triggering moments demonstrated large changes in the paraspinal muscle activation patterns. Similarly, tension–relaxation

induced in the lumbar viscoelastic tissues during passive cyclic flexion–extension resulted in pronounced increases in muscular activity during subsequent active movement. We can speculate from these findings that the motor control system of the spine regularly monitors the moments developed in the viscoelastic tissues for any given movement, and uses this information to activate or inhibit the spinal musculature to meet the demands for executing the movement and maintenance of spinal stability. Precisely timed reflexive excitation and inhibition of spinal muscles were triggered as required and not necessarily by a hard-wired ligamento-muscular reflexive loop.

While such an assertion is reasonable and has now been confirmed in the feline and human models, the question remains as to why the first 2–3 h after static loading were not compensated, potentially increasing the risk to instability and injury. This question should be addressed in future investigations of the NNZs and the parallel compensatory mechanisms of the spine.

5. Conclusions

Based on the data contained and its implication, the following could be concluded:

1. A sequence of static lumbar loading/rest at 1:1 ratio and at moderate load elicits a significant increase in the displacement and tension neuromuscular neutral zones concurrent with a decrease of paraspinal muscular activity.
2. A reduction in spinal stability composed of viscoelastic tissues laxity as well as deficient activation of the musculature exists post-static loading.
3. The laxity of the viscoelastic tissues persists for 7 h before full recovery, whereas significantly early activation of the musculature at a substantially higher magnitude than normal is observed 2–3 h post-static loading.
4. The presence of a motor control compensatory mechanism, more complex than a simple reflex is confirmed and supported by evidence of complex activation or inhibition as required by the moments developed in the spine.
5. The 2–3 h immediately post-static loading finds the lumbar spine with deficient stability and exposes it to high-risk of injury.

It is expected that the new finding available from this study will shed additional light on the issues revolving spinal stability and its motor control, as well as in our understanding of low back disorders and their prevention.

Acknowledgement

This work was supported by Grant R01-OH-007622 from the National Institute of Occupational Safety and Health.

References

Adams, M., 2007. Re: Spine stability: the six blind men and the elephant. Clin. Biomech. 22, 486, author reply 7–8.

Adams, M.A., Dolan, P., Hutton, W.C., 1987. Diurnal variations in the stresses on the lumbar spine. Spine 12, 130–137.

Courville, A., Sbriccoli, P., Zhou, B.H., et al., 2005. Short rest periods after static lumbar flexion are a risk factor for cumulative low back disorder. J. Electromyogr. Kinesiol. 15, 37–52.

Dickey, J., McNorton, S., Potvin, J., 2003. Repeated spinal flexion modulates the flexion–relaxation phenomenon. Clin. Biomech. 18, 783–789.

Eversull, E., Solomonow, M., Bing He Zhou, E.E., et al., 2001. Neuromuscular neutral zones sensitivity to lumbar displacement rate. Clin. Biomech. 16, 102–113.

Granata, K.P., Marras, W.S., 2000. Cost-benefit of muscle cocontraction in protecting against spinal instability. Spine 25, 1398–1404.

Granata, K.P., Marras, W.S., Davis, K.G., 1999. Variation in spinal load and trunk dynamics during repeated lifting exertions. Clin. Biomech. 14, 367–375.

Granata, K.P., Rogers, E., Moorhouse, K., 2005. Effects of static flexion–relaxation on paraspinal reflex behavior. Clin. Biomech. 20, 16–24.

Hedman, T.P., Fernie, G.R., 1995. In vivo measurement of lumbar spinal creep in two seated postures using magnetic resonance imaging. Spine 20, 178–183.

Hoogendoorn, W.E., Bongers, P.M., de Vet, H.C., et al., 2000. Flexion and rotation of the trunk and lifting at work are risk factors for low back pain: results of a prospective cohort study. Spine 25, 3087–3092.

Keller, T.S., Hansson, T.H., Holm, S.H., et al., 1988. In vivo creep behavior of the normal and degenerated porcine intervertebral disk: a preliminary report. J. Spinal Disord. 1, 267–278.

Krajcarski, S., Wells, R., 2006. The time variation pattern of mechanical exposure and the reporting of low back pain. Theoret. Issues Ergon. Sci., 1–27.

LaBry, R., Sbriccoli, P., Zhou, B.H., et al., 2004. Longer static flexion duration elicits a neuromuscular disorder in the lumbar spine. J. Appl. Physiol. 96, 2005–2015.

Li, L., Patel, N., Solomonow, D., Le, P., Hoops, H., Gerhardt, D., Johnson, K., Zhou, B., Lu, Y., Solomonow, M., 2007. Neuromuscular response to cyclic lumbar twisting. Hum. Factors 49, 820–829.

Little, J.S., Khalsa, P.S., 2005. Human lumbar spine creep during cyclic and static flexion: creep rate, biomechanics, and facet joint capsule strain. Ann. Biomed. Eng. 33, 391–401.

Marras, W.S., 2000. Occupational low back disorder causation and control. Ergonomics 43, 880–902.

McGill, S.M., Brown, S., 1992. Creep response of the lumbar spine to prolonged full flexion. Clin. Biomech. 7, 43–46.

Olson, M.W., Li, L., Solomonow, M., 2004. Flexion–relaxation response to cyclic lumbar flexion. Clin. Biomech. 19, 769–776.

Olson, M., Solomonow, M., Li, L., 2006. Flexion–relaxation response to gravity. J. Biomech. 39, 2545–2554.

Olson, M.W., Li, L., Solomonow, M. Interaction of viscoelastic tissue compliance with lumbar muscles during passive cyclic flexion–extension. J. Electromyogr. Kinesiol. in press.

Panjabi, M.M., 1992. The stabilizing system of the spine. 2. Neutral zone and instability hypothesis.. J. Spinal Disord. 5, 390–397.

Panjabi, M.M., 1996. Low back pain and spinal stability. In: Weinstein, J.N., Gordon, S.L. (Eds.), Low back pain: a scientific and clinical overview. American Academy of Orthopedic Surgeons, Rosemont, IL. pp. 367–384.

Punnett, L., Fine, L.J., Keyserling, W.M., et al., 1991. Back disorders and nonneutral trunk postures of automobile assembly workers. Scand. J. Work Environ. Health 17, 337–346.

Reeves, N.P., Narendra, K.S., Cholewicki, J., 2007. Spine stability: the six blind men and the elephant. Clin. Biomech. 22, 266–274.

Sbriccoli, P., Solomonow, M., Zhou, B.H., et al., 2004a. Static load magnitude is a risk factor in the development of cumulative low back disorder. Muscle Nerve 29, 300–308.

Sbriccoli, P., Yousuf, K., Kupershtein, I., et al., 2004b. Static load repetition is a risk factor in the development of lumbar cumulative musculoskeletal disorder. Spine 29, 2643–2653.

Sbriccoli, P., Solomonow, M., Zhou, B.H., et al., 2007. Work to rest durations ratios exceeding unity are a risk factor for low back disorder; a feline model. J. Electromyogr. Kinesiol. 17, 142–152.

Shin, G., Mirka, G., 2007. An in vivo assessment of the low back response to prolonged-flexion; interplay between active & passive tissues. Clin. Biomech. 22, 965–971.

Solomonow, M., Zhou, B.H., Baratta, R.V., et al., 1999. Biomechanics of increased exposure to lumbar injury caused by cyclic loading: Part 1. Loss of reflexive muscular stabilization. Spine 24, 2426–2434.

Solomonow, M., Zhou, B., Baratta, R., Lu, Y., Zhu, M., Harris, M., 2000. Bi-exponential recovery model of lumbar viscoelastic laxity and reflexive muscular activity after prolonged cyclic loading. Clin. Biomech. 15, 167–175.

Solomonow, M., Eversull, E., He Zhou, B., et al., 2001. Neuromuscular neutral zones associated with viscoelastic hysteresis during cyclic lumbar flexion. Spine 26, E314–E324.

Solomonow, M., Baratta, R.V., Banks, A., et al., 2003a. Flexion–relaxation response to static lumbar flexion in males and females. Clin. Biomech. 18, 273–279.

Solomonow, M., Baratta, R.V., Zhou, B.H., et al., 2003b. Muscular dysfunction elicited by creep of lumbar viscoelastic tissue. J. Electromyogr. Kinesiol. 13, 381–396.

Stubbs, M., Harris, M., Solomonow, M., Zhou, B., Lu, Y., Baratta, R., 1998. The ligamento-muscular protective reflex in the lumbar spine. J. Electromyogr. Kinesiol. 8, 197–204.

Twomey, L., Taylor, J., 1982. Flexion creep deformation and hysteresis in the lumbar vertebral column. Spine 7, 116–122.

van Dieen, J.H., Selen, L.P., Cholewicki, J., 2003. Trunk muscle activation in low-back pain patients, an analysis of the literature. J. Electromyogr. Kinesiol. 13, 333–351.